water

MDPI

Article

Groundwater Age and Origin and Its Relation with Anthropogenic and Climatic Factors

Usman Iqbal [1], Ghulam Nabi [1,*], Mudassar Iqbal [1], Muhammad Masood [1], Abu Bakar Arshed [1], Muhammad Saifullah [2] and Muhammad Shahid [3,*]

[1] Centre of Excellence in Water Resources Engineering, University of Engineering and Technology, Lahore 54890, Punjab, Pakistan; engr.usman25@yahoo.com (U.I.); mudassar@cewre.edu.pk (M.I.); masood@cewre.edu.pk (M.M.); abubakararshad432@gmail.com (A.B.A.)
[2] Department of Agricultural Engineering, Muhammad Nawaz Sharif University of Agriculture Multan, Multan 66000, Punjab, Pakistan; muhammad.saifullah@mnsuam.edu.pk
[3] Department of Civil and Environmental Engineering, Brunel University, Uxbridge, Middlesex, London UB8 3PH, UK
* Correspondence: gnabi60@yahoo.com (G.N.); m.shahid@nice.nust.edu.pk or muhammad.shahid@brunel.ac.uk (M.S.)

Abstract: Groundwater plays a major role in addressing the worldwide problem of water scarcity and food security. With a growing population and increasing urbanization, there is a rising demand for groundwater to meet agricultural and domestic water needs. A variety of advanced approaches are necessary to sustain groundwater management. This study investigated the age and origin of groundwater, as well as its relationship with anthropogenic and climatic factors. Stable isotopes were used, namely oxygen-18 (^{18}O) and deuterium (^{2}H) for the estimation of groundwater origin and radioactive isotopes of Tritium (^{3}H) for the estimation of its age. The investigation of stable isotopes revealed that the aquifer is predominantly influenced by river water, with a minor contribution from rainwater. Furthermore, the analysis of radioactive isotopes revealed that the groundwater age ranges from 5 to 50 years old in most areas. Older groundwater is predominantly found in urban areas, while younger groundwater is present in agricultural and woodland regions. However, the presence of "old" water in the upper groundwater layers in urban areas is attributed to over-abstraction and limited natural recharge. The primary climatic factor that governs the age and origin of groundwater is rainfall upstream of the study area, which directly contributes to the river flows. The rainfall is high in the east but, due to urbanization, recharge is decreased. Consequently, old and river recharge groundwater is found in this area. These observations underscore the unsustainable and alarming use of groundwater in urban areas.

Keywords: anthropogenic and climatic factors; isotopes; water quality; NDVI; groundwater age; groundwater origin

Citation: Iqbal, U.; Nabi, G.; Iqbal, M.; Masood, M.; Arshed, A.B.; Saifullah, M.; Shahid, M. Groundwater Age and Origin and Its Relation with Anthropogenic and Climatic Factors. *Water* **2024**, *16*, 287. https://doi.org/10.3390/w16020287

Academic Editor: Paolo Madonia

Received: 12 December 2023
Revised: 2 January 2024
Accepted: 10 January 2024
Published: 15 January 2024

1. Introduction

Understanding and monitoring water resources is challenging due to their heterogeneity and composite boundary conditions [1]. The hydrological cycle boundary conditions continuously vary because of the influence of anthropogenic and climatic factors, which require multi-disciplinary research. This is especially the case when considering surface and subsurface water resources [2,3]. Due to the rapidly expanding population, surface water has become insufficient to meet requirements; hence, groundwater is essential for addressing the deficiencies in surface water availability and satisfying the increasing demand for water [3,4]. The quality and quantity of groundwater are determined mainly by natural processes, anthropogenic activities, and atmospheric inputs [5,6]. Anthropogenic factors mainly include industrialization; the overexploitation of aquifers; rapid population

growth; agricultural pesticides; land use pattern variation; and the disposal of urban, domestic, and industrial waste [3,7]. The groundwater recharge system is directly influenced by climatic factors such as precipitation, temperature, evapotranspiration (ET), and soil moisture [2,4]. Consequently, such studies are critical to ensure the prolonged management of groundwater resources by regulating their diminishing quality and quantity.

Various studies used the stable and radioactive isotopes to study groundwater origin and flow dynamics [8,9], groundwater age [10,11], groundwater recharge [12,13], seasonal groundwater recharge [14,15], and examine surface and groundwater interaction [16]. Groundwater age on Earth is generally unknown and varies from centuries to millions of years in arid regions [9] and months to years in humid and semi-humid regions [10]. Groundwater from different ages also supply the same aquifer, complicating the understanding of groundwater age [11]. Groundwater can be categorized as modern groundwater, less than 50 years old; young groundwater, recharged in the past 50–100 years; and old groundwater, recharged in more than 100 years ago11.

Traditionally, two methods have been widely used to assess groundwater age, i.e., numerical simulation and radioisotope tracers [17]. The radioactive isotopes of carbon (^{14}C) and hydrogen (^{3}H) in water are used to estimate the particular water's age, depending on its half-life [18]. However, groundwater origin and recharge source remain fundamental questions [19]. Groundwater can originate from precipitation, rivers, canals, and neighboring aquifers [20–22]. In addition, stable isotopes of oxygen (^{18}O) and hydrogen (^{2}H) in water vapors, rainwater, and river water show a distinct trend across the area and provide a convenient approach to understanding groundwater origin [23,24]. The isotope composition in groundwater has been compared with the precipitation signal, and its deviations indicate the source of recharge (origin) water or a specific precipitation type [25]. In addition, many researchers have also used various geographical and statistical techniques for assessing groundwater quality trends to protect groundwater resources at the regional level [26,27].

Numerous studies have examined groundwater by isotope analysis; however, most consider only old groundwater [10,28,29], and a few only used isotope analysis for the shallow aquifer [12,14]. Additionally, satellite images of coarser resolution for land characterization with limited number of isotope samples at shallow depths were analyzed [30–32]. By integrating isotopic analysis into groundwater management strategies, Pakistan can have less uncertainty about the long-term availability and quality of this essential resource, supporting agricultural productivity, human health, and overall economic development. However, some studies, such as those conducted by Hussain et al. [33] in Islamabad and by Ahmad et al. [34] in Lahore, consider limited samples at shallow depths of up to 5m using stable isotopes in precipitation. Consequently, the isotopes in groundwater at varying depths still need to be explored. Stable isotope measurements and their investigations in precipitation are still lacking in the region. Hence, the use of isotopes and fine resolution satellite images is both essential and advantageous in order to accurately ascertain the origin and age of groundwater.

This research will be helpful in answering various scientific research questions: what is the relationship between groundwater and isotopes, and how are isotopic analyses helpful in managing groundwater resources? The present study aims to investigate the groundwater age and origin for sustainable groundwater management considering the influence of climatic and anthropogenic factors. Policymakers and water resource managers can make decisions regarding sustainable groundwater use, allocation, conservation, and this study can also provide valuable insights for the effective management of groundwater resources.

2. Materials and Methods

2.1. Study Area

This study was performed in the Lower Bari Doab Indus Basin, Punjab, Pakistan. It comprises the areas of Lahore and Kasur districts and has a coverage of 4279 km^2. The area serves as a food hub of the country, as maize, potato, paddy, vegetables, and wheat are

common crops grown to feed more than 10 million inhabitants in this region. The climate is tropical, with a hot summer season and a cold winter. Three distinct seasons exist in the study region: winter, summer, and the rainy season [35]. The average annual rainfall is 423 mm and 70% of this rainfall is concentrated in June to August. The temperature varies from 5 °C in winter to 41 °C in summer. Two rivers, Ravi and Sutlej, flow north and south of the area, respectively (Figure 1). The soil is alluvial for the late Pleistocene, formed by the river Ravi and Sutlej flood plains. These consist of clay, sand, and silt, and the thickness of clay increases as the distance increases from the riverbed. Surface elevation varies from 257 m to 161 m from south to north. The slope is generally flat towards the south and southwest, with an average rate of (1:4000).

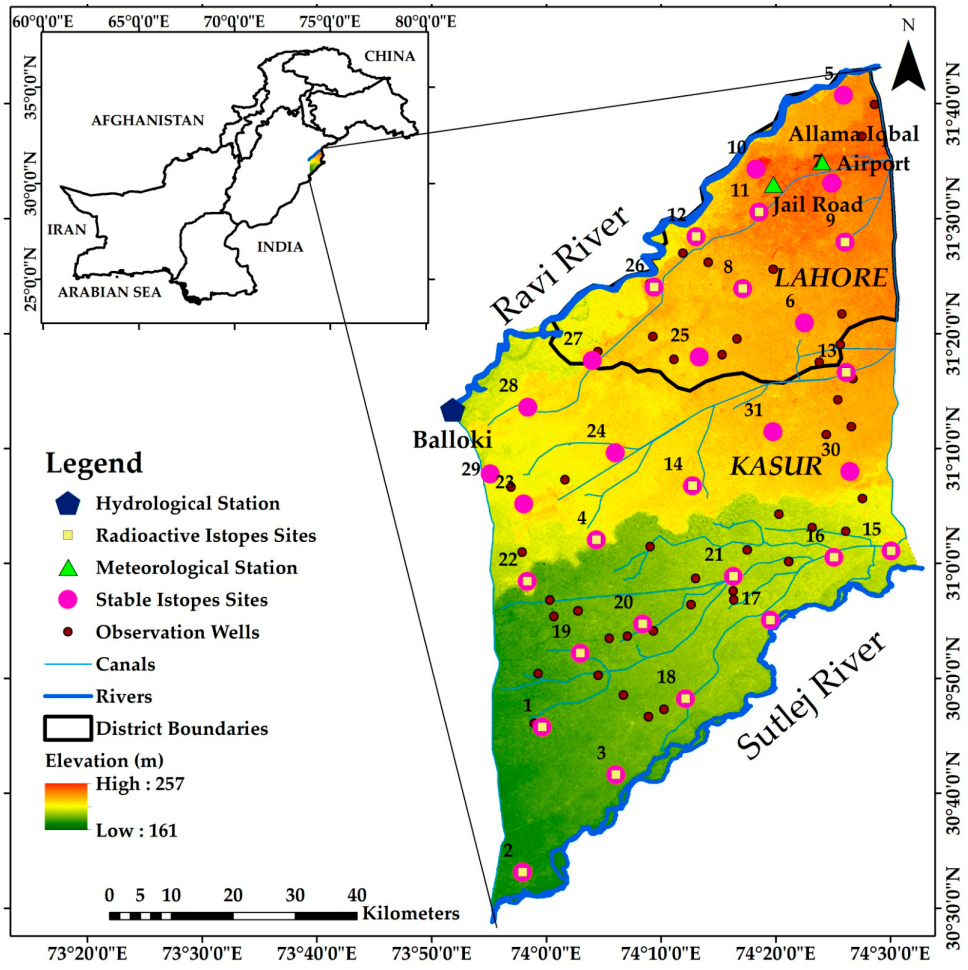

Figure 1. Geographical and hydrographic location of the study area, with topographic and sampling site information.

2.2. Datasets

2.2.1. Climatic Data

Climatic data, including mean monthly rainfall, maximum (Tmax), and minimum temperature (Tmin) were gathered from the Pakistan Meteorological Department (PMD) for the period of 2011 to 2021. Previous studies have consistently relied on climatic data obtained from the PMD. The consistency of using this data across multiple studies ensures the reliability and comparability of findings related to groundwater management in Pakistan [36–39].

2.2.2. Spatial Data

Landsat 8 OLI (operational land imager) data of May 2021 was provided by the USGS (United States Geological Survey) Earth Explorer database. The nominal spacecraft height is 705 km, and the scene size for Landsat 8 is 185 km cross track by 180 km long track. Accuracy in cartography is 12 m [39]. The presence of cloud cover posed a challenge in generating high-quality images. To address this issue, an algorithm was implemented on the USGS database, which selected the optimal pixel value with cloud cover, and other collection errors below 5%. The Normalized Vegetation Index (NDVI) was calculated using nine spectral bands in the dataset, each with a spatial resolution of 30 m.

2.2.3. Isotopic Data

The groundwater samples were collected from 31 wells, as shown in Figure 1, at various depths. Prior to collecting the samples for isotope analysis, the casing was thoroughly purged to ensure its cleanliness. These samples were collected into 1000 mL amber glass air-tight bottles to avoid evaporation. Stable isotopes were analyzed by liquid water isotope analyzer (LWIA) and isotope ratio mass spectrometer (IRMS). LWIA was used for samples with EC $\leq$ 1500 µS/cm, and for samples with EC > 1500 µS/cm, IRMS was used. Radioactive isotopes were analyzed by refrigerated liquid scintillation analyzer (RLSA). Stable isotopes were analyzed in all samples, and radioactive isotopes were analyzed in 19 samples, as presented in Figure 1.

The data from the precipitation's isotopes were gathered from the International Atomic Energy Agency (IAEA) and the Global Network for Isotopes in Precipitation (GNIP) database (https://nucleus.iaea.org/wiser/index.aspx (assessed on 15 May 2023)). The isotopic data of surface water (River Ravi), at Balloki headwork hydrological station, was collected from the database of the Global Network for Isotopes in River (GNIR) (https://www.iaea.org (assessed on 20 May 2023)). GNIP and GNIR are a globally operating network that systematically gather isotope data from groundwater and surface water [40].

2.2.4. Groundwater Quality and Depth to the Water Table Data

A total of 46 observation wells (presented in Figure 1) were selected to gather groundwater quality and water table depth data for the 2003–2020 period from the Punjab Irrigation Department (PID), Pakistan. The selection process prioritized the completeness and consistency of the records to ensure the highest quality of data. Groundwater quality data, including sodium adsorption ratio (SAR), residual sodium carbonate (RSC), and electrical conductivity (EC), was obtained to assess water quality trends. Additionally, the PID provided data on the depth to the water table (DWT) to analyze groundwater levels.

2.3. Methodology

2.3.1. Groundwater Age

The age of groundwater was estimated by the Tritium method [20,41]. Tritium, with a 12.32-year half-life, is commonly used as a dating tool for groundwater within the recent to 100-year age range [42]. Tritium is considered an excellent and conservative tracer because of its chemical property to be a part of the water molecule. Correspondingly, it is not impacted by hydro-chemical or biological interactions and solely decays through radioactivity. Taking into consideration travel time through the unsaturated zone is one benefit of using Tritium ages instead of gas ages. This is due to the fact that the "Tritium clock" begins when water seeps into the earth and separates from air moisture. In contrast, gas methods only define the travel time from the water table to the sampling point, excluding travel time through the unsaturated zone due to gas exchange in that zone. The increasing difference in Tritium signature between rainwater and old groundwater allows for robust differentiation between young and older groundwater. In past decades, Tritium concentration changes were due to the introduction of Tritium into groundwater systems through rainfall as a result of the 1950s and 1960s nuclear weapons testing. The concentration of Tritium increased

significantly during this period, reaching levels ranging from 10 to over 2000 Tritium Units (TU) (International Atomic Energy Agency (IAEA), 1983). The decay of remaining Tritium can be used straightforwardly for groundwater dating in single Tritium measurements.

Mass spectrometry techniques were used to measure Tritium [43,44]. For the measurement of Tritium concentration, groundwater samples were tested in the Pakistan Institute of Nuclear Science and Technology (PINSTECH), Islamabad. Groundwater age was estimated according to the ranges of TU, presented in Table 1, which were provided by PINSTECH.

Table 1. Tritium Units (TU) ranges for groundwater age.

TU	Groundwater Age
<5	>50 years
5–8	10–50 years
8–12	5–10 years
12–30	Fusion explosion Tritium
>30	Recharge in 1960–1970

2.3.2. Groundwater Origin

Deuterium (^{1}H and ^{2}H) and Oxygen-18 (^{16}O and ^{18}O) are the essential stable isotopes that form an integral part of a water molecule. These isotopes are commonly used to identify groundwater sources [20]. For oxygen-18, it has a ratio of ^{18}O and ^{16}O; for deuterium, it has a ratio of ^{2}H and ^{1}H. The isotope concentrations were measured by gas source mass spectrometry in PINSTECH, with an upper limit of standard deviation $<\pm 1\%$ and $<\pm 0.1\%$ for ^{18}O and ^{2}H, respectively. For the ^{18}O isotopes, the equilibration method involved using 200 microliters of water samples in a vial. The headspace of the vial was purged with a gas mixture comprising 99.5% helium (He) and 0.5% carbon dioxide (CO_2). To fill the vial with the mixed gas, a needle with two capillaries was employed in a flush and fill process that took approximately 15 min. One capillary introduced the mixed gas into the vial, while the other removed the gas from the headspace. This allowed the oxygen atoms of the CO_2 gas in the headspace to equilibrate with the oxygen atoms of the water molecules. In the equilibration method for the ^{2}H isotopes, the mixed gas comprised a ratio of 98% helium (He) and 2% hydrogen (H_2). Platinum alumina rods were present in the vial, serving as a catalyst. The ratio of heavy isotopes to light ones is presented in Delta (δ) notation.

$$\text{Delta}(\delta) = \frac{R_{sample} - R_{standard}}{R_{standard}} \times 1000 \quad (1)$$

where R_{sample} represents the isotopes in the sample and $R_{standard}$ represents in standard/reference (per mil or %) relative to the Vienna standard mean ocean water (VSMOW). The ratios of heavy isotopes to lighter isotopes were determined using Equation (1). These ratios were then compared to the data from GNIP and GNIR, with reference to Table 2 provided by PINSTECH.

Table 2. Groundwater origin based on stable isotopes values.

Groundwater Origin	^{18}O (%)	^{2}H (%)
Rain water	>-5.2	>-31
Major rainwater and some terraces of river water	-5.2 to -6.2	-31 to -39
Major river water and some terraces of rainwater	-6.2 to -7.2	-39 to -48
river water	<-7.2	<-48

2.3.3. Normalized Difference Vegetation Index (NDVI)

NDVI, a widely used vegetation index, measures and quantifies greenness and vegetation density captured in a satellite image. It has been employed since the 1970s to monitor crop biomass, characterize land, and identify changes in land use and landcover [45–47].

In this study, various combinations of Green, Red, and Near Infrared (NIR) bands were created to form a Red, Green, and Blue (RGB) color image to attribute to the different land cover. The RGB image serves as a standard representation for infrared images [48]. The classification of the image was based on calculating the NDVI values by following equation.

$$NDVI = \frac{NIR - RED}{NIR + RED} \tag{2}$$

The *NDVI* is an index that relies on the spectral reflectance of ground surface features, with each feature exhibiting its unique reflectance characteristics that vary with wavelength. The *NDVI* value ranges from −1 to +1. The existence of healthy vegetation is indicated by a higher *NDVI* value, while urban areas or bare terrain are indicated by a lower value [45].

2.3.4. Mann–Kendall (MK) Test

The nonparametric Mann–Kendall test [49,50] was utilized to identify the trends of water quality and DWT. MK test is commonly used to identify trends for the time-series data in groundwater studies [26,51,52] due to its normal distribution and insensitivity to outliers in time-series data. The MK test statistic (S) is given by:

$$S = \sum_{k=1}^{n-1} \sum_{j=k+1}^{n} sgn(X_j - X_k) \tag{3}$$

$$sgn(X_j - X_k) = \begin{Bmatrix} if(X_j - X_k) < 0; & then & -1 \\ if(X_j - X_k) = 0; & then & 0 \\ if(X_j - X_k) > 0; & then & 1 \end{Bmatrix} \tag{4}$$

where X_j and X_k are the successive data values at times j and k and n is the dataset's overall length. In time series data, positive S values show an upward (growing) trend, while negative S values show a downward (decreasing) trend. The test is performed with a normal distribution ($\sigma^2 = 1$) and mean ($\mu = 0$) for datasets with $n > 10$ [53], with expectation (E) and variance (Var) as follows:

$$E[S] = 0 \tag{5}$$

$$Var(S) = \frac{n(n-1)(2n+5) - \sum_{k=1}^{p} t_k(t_k-1)(2t_k+5)}{18} \tag{6}$$

where the symbol ($\sum$) denotes the total of all linked groups and t_k is the number of tied values in the qth group. If there are no connected groups in the data, the summary course could be disregarded. The following formula is used to determine the value of the standardized test statistic (Z_{MK}) following the computation of variance Var (S) from Equation (6).

$$Z_{MK} = \begin{cases} \frac{S-1}{\sqrt{VAR(S)}}, & if\ S > 0 \\ 0, & if\ S = 0 \\ \frac{S+1}{\sqrt{VAR(S)}}, & if\ S < 0 \end{cases} \tag{7}$$

The consistent Z_{MK} values are used to calculate the degree of variation and have a normal distribution with a mean of "0" and a variance of "1". The null hypothesis, or H_0, is verified using the test statistic. Z_{MK} greater than $Z_{\alpha/2}$ indicates a substantial trend in the data set. At a confidence level of α = 10%, the value of Z_{MK} is compared with the two-tailed test's normal distribution table. In the two-tailed test, the null hypothesis (H_0) is agreed for no trend if the computed value of Z_{MK} falls between—$Z_{1-\alpha/2}$ and $Z_{1-\alpha/2}$, so H_1 is rejected. The study estimates groundwater time series data trends at 1%, 5%, and 10% significance levels.

3. Results

3.1. Land Characterization

The classification process involved mapping and labeling the classes based on color. As depicted in Figure 2, the images were categorized into four groups, based on their NDVI values. In this classification, the NDVI ratio was calculated using threshold values, and the pixels of the image were subsequently classified. The waterbodies exhibited the minimum NDVI values, ranging between −0.11 and −0.05. The non-vegetation class, which included urban areas, displayed medium NDVI ranging from 0.09 to 0.11. The agricultural area fell under the moderate NDVI value range. The high NDVI values were associated with dense vegetation and woodlands. NDVI ratios ranged between 0.27 and 0.35, indicate moderated NDVI values and, were assigned to the vegetation class. Pixels with NDVI ratios exceeding 0.35 were assigned to the dense vegetation and woodlands class.

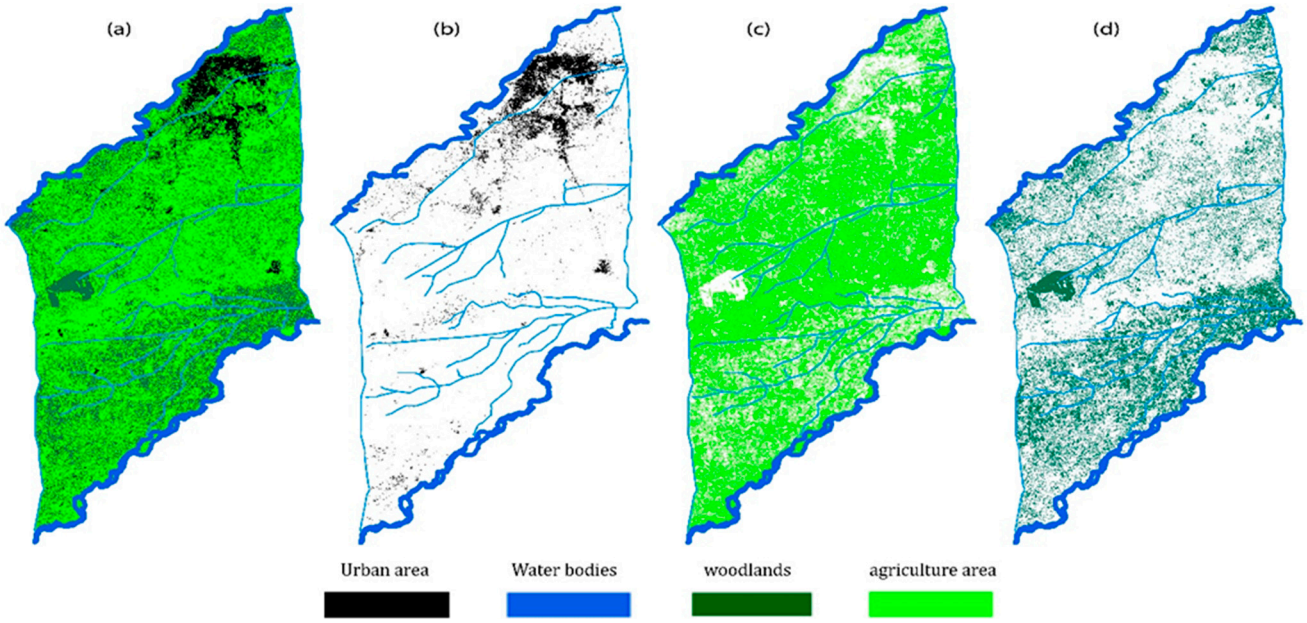

Figure 2. (**a**) NDVI-based classification representing water bodies, urban areas, agriculture areas, and woodlands; (**b**) blue color represents water bodies, and black color represents urban areas; (**c**) the light green color represents agriculture areas; and (**d**) the dark green color represents the woodlands in the study area.

A comparison of the four NDVI classes is displayed in Figure 2. Figure 2a primarily represents water bodies with a 16% area. Water bodies like rivers bounded the study areas from north to south, and canals flow along the rivers to irrigate agricultural lands. Figure 2b represents the urban area. The dominant urban area on the river Ravi's eastern bank extended towards the river's downstream side. The scattered urban area layouts along the canals comprise 33% of the total area. Figure 2c presents complex cultivations—agriculture mixed with natural vegetation covers 36% of the area. Figure 2d shows woodlands and dense vegetation, which covered 15% of the area. The woodlands were mainly present along the west bank of the river Sutlej. The discontinuous dense vegetation cover is also present along the canal's branches.

3.2. Groundwater Age

The radioisotope Tritium (^{3}H) was analyzed in nineteen samples of 9 m–167 m depth. The values of Tritium ranged from 4.73 to 11.77 TU. Table 3 presents the analytical data of radioisotopes concentration in the samples of groundwater. Figure 3a,b presents groundwater age distribution in urban and agricultural areas. The area where 5–10-year-old groundwater is present is in green color, the area where the groundwater age is 10–50-years-old

is in yellow, and the area in which the groundwater age is more than 50 years is in red, as presented in Figure 3. The distribution of ^{3}H in groundwater varies and reflects the intricate vertical pathways connecting the topsoil surface with spatially dispersed aquifers. Consequently, the concentrations of Tritium and, thus, the age of the groundwater, do not uniformly spatially distribute due to the potential variability in the topography. The variability in age also indicates that the fluctuation in annual recharge and discharge from aquifers differs in urban and agricultural areas. Groundwater in the dense urban area is the oldest water, more than 50 years, found in the study area. The oldest water is located in the center of the research region, far from rivers and canals, as shown in Figure 3a. The analysis of Tritium ^{3}H isotopes revealed that, in agricultural areas and woodlands, the groundwater age is 5–50 years, as shown in Figure 3b.

Table 3. Isotope concentration with geographical location in groundwater samples.

Sample ID	Latitude (DMS)	Longitude (DMS)	Depth (m)	Oxygen-18 ^{18}O (%)	Deuterium ^{2}H (%)	Tritium ^{3}H (TU)
1	31°23′15″	74°34′34″	91.44	−6.87	−44.71	8.23
2	31°24′43″	74°35′04″	25.91	−6.06	−41.89	9.01
3	31°32′11″	74°35′54″	137.16	−7.35	−51.85	8.55
4	31°35′35″	74°33′18″	25.91	−8.59	−55.34	10.49
5	31°42′11″	74°28′7.47″	18.29	−9.62	−60.4	-
6	31°20′57″	74°22′31″	27.43	−5.28	−35.05	-
7	31°45′02″	74°42′15″	27.43	−5.31	−36.5	-
8	31°29′29″	74°35′08″	121.92	−7.1	−45.79	4.73
9	31°37′45″	74°32′35″	106.68	−8.17	−52.94	10.29
10	31°40′09″	74°31′16″	30.48	−7.95	−48.87	-
11	31°35′20″	74°25′27″	152.40	−8.2	−50.247	10.54
12	31°34′19″	74°18′18″	167.64	−8.73	−53.25	10.14
13	31°30′34″	74°18′34″	15.24	−8.06	−53.12	10.81
14	31°28′26″	74°13′04″	18.29	−9.65	−59.73	11.77
15	31°17′39.33″	74°30′39.52″	9.14	−8.2	−55.07	10.16
16	31°13′40″	74°30′45.6″	45.72	−8.07	−53.63	10.57
17	31°03′40″	74°31′47″	42.67	−6.57	−41.42	7.69
18	31°00′32″	74°25′06″	44.20	−9.49	−60.62	8.27
19	30°55′03″	74°19′33″	30.48	−8.98	−59.51	8.15
20	30°48′13″	74°12′09″	73.15	−9.6	−64.51	9.52
21	30°52′12″	74°02′59″	30.48	−8.82	−57.68	10.51
22	30°58′26″	73°58′21″	30.48	−7.59	−48.36	8.93
23	31°05′11″	73°58′03″	21.34	−7.19	−49.9	-
24	31°09′37″	74°06′02″	22.86	−7.77	−53.15	-
25	31°17′58″	74°13′20″	24.38	−6.4	−42.69	-
26	31°24′03″	74°09′24″	106.68	−8.42	−53.24	9.35
27	31°17′39″	74°04′01″	36.58	−9.03	−57.31	-
28	31°13′35″	73°58′24″	19.81	−8.78	−56.13	-
29	31°07′48″	73°55′07″	45.72	−7.88	−52.95	-
30	31°08′0.19″	74°26′29.18″	28.96	−8.92	−57.29	-
31	31°11′27.74″	74°19′46.12″	24.38	−5.23	−36.17	-

3.3. Groundwater Origin

The stable isotopes, oxygen-18 (^{18}O) and deuterium (^{2}H), were examined in thirty-one groundwater samples. Overall ^{2}H values ranged from −35.05% to −64.51% and ^{18}O ranged between −5.23% and −9.65%. Long-term annual multi-correlations show that 60% of ^{18}O is directly linked with temperature; however, 50%, and 48% of ^{18}O are indirectly linked with humidity and precipitation, respectively. The long-term trend of isotopes in rainfall is the so-called Local Meteoric Water Line (LMWL), which was developed as in previous studies [33]. The analytical data of stable isotopes in the samples of groundwater is also presented in Table 3. Based on the findings shown in Figure 4, it was found that 71% of the groundwater samples are located below the LMWL, indicating that the groundwater in this

area is primarily recharged by river water. Additionally, 16% of the groundwater samples aligned below the LMWL contain a mixture of mostly river water and some terraces of rainwater. Furthermore, 13% of the groundwater samples aligned above the LMWL show a recharge of mostly rainwater, along with some terraces of river water. It is important to note that none of the samples consisted solely of rainwater.

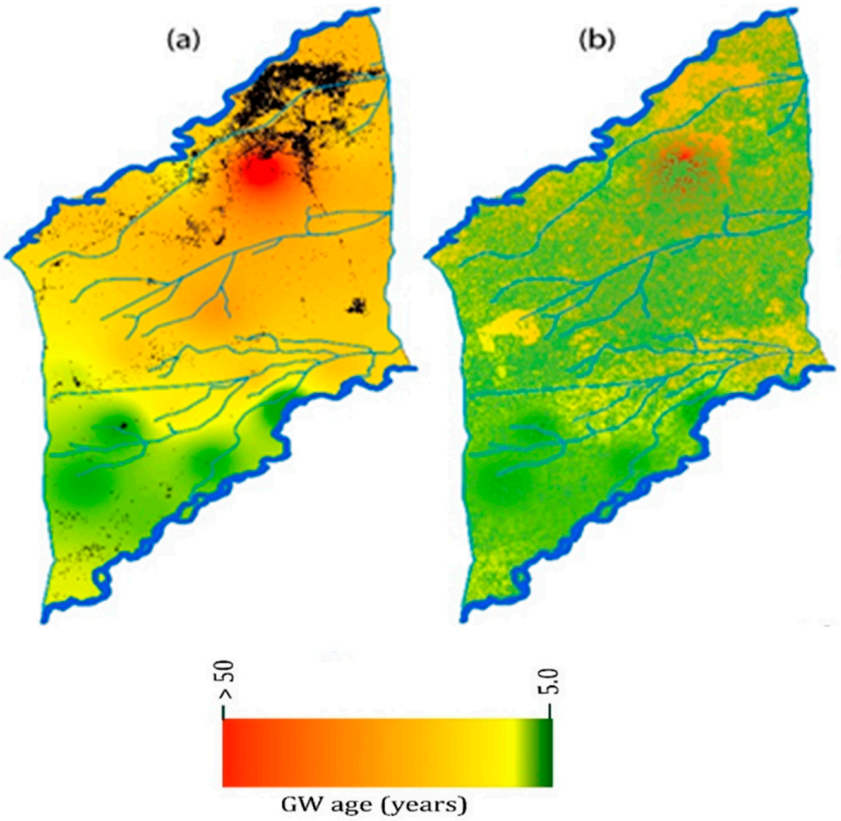

Figure 3. Distribution of groundwater age in (**a**) urban areas and (**b**) agricultural areas.

Approximately two-thirds of the study area relies on river water for aquifer recharge, while the remaining one-third receives both rainwater and river water recharge.

The maps regarding the distribution of groundwater origin are presented in Figure 5. The findings indicate that the aquifer in urban areas is solely recharged by river water, while the agricultural areas receive recharge mainly from rainwater and river water. Figure 5a shows that river water recharges its adjacent areas, and as the distance increases from the river, the percentage of river water in groundwater decreases. On the other hand, the contribution of rainwater to the aquifer is relatively small, as depicted in Figure 5b.

The relationship between elevation and stable isotopes in recharged water is depicted in Figure 6. The figures illustrate that areas of lower elevation exhibit higher concentrations of heavy isotopes, while lighter isotopes become more concentrated with increasing elevation. This pattern can be explained by the tendency of lighter isotopes to settle at higher elevations. Additionally, the contribution of river water is observed in both high and low elevated areas, as high-altitude regions contain lighter stable isotopes that contribute to the river flow, which moves from high to low altitude areas. The maps also indicate that although there may be some evaporation of lighter isotopes in the groundwater recharged from river water, its overall impact on the isotopic distribution is minimal.

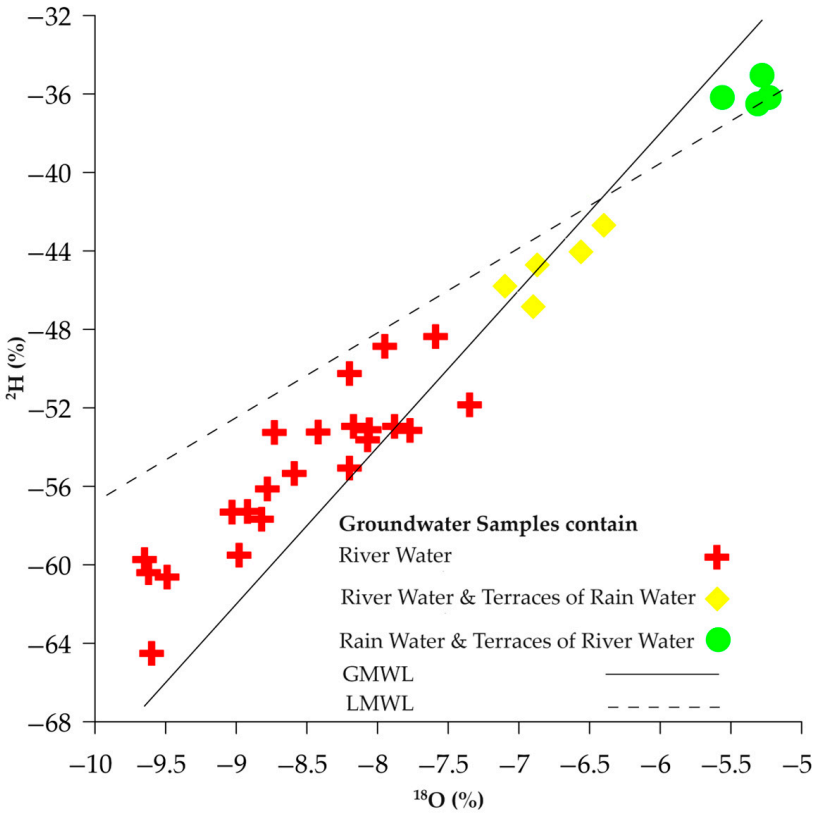

Figure 4. Bivariate diagram of stable isotope (^{2}H, ^{18}O), Global Meteoric Water Line (GMWL) developed by ^{2}H (%) = 8 × ^{18}O (%) + 10 [54], Local Meteoric Water Line (LMWL) developed based on annual weighted mean data of Balloki hydrological station (2002–2016).

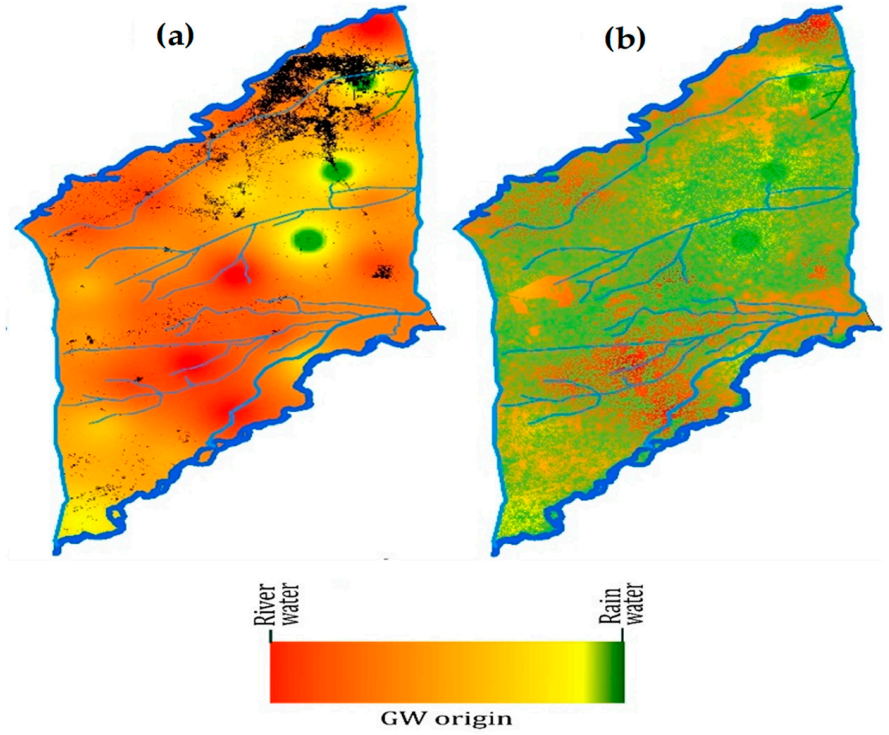

Figure 5. Distribution of groundwater origin in (**a**) urban areas and (**b**) agricultural areas.

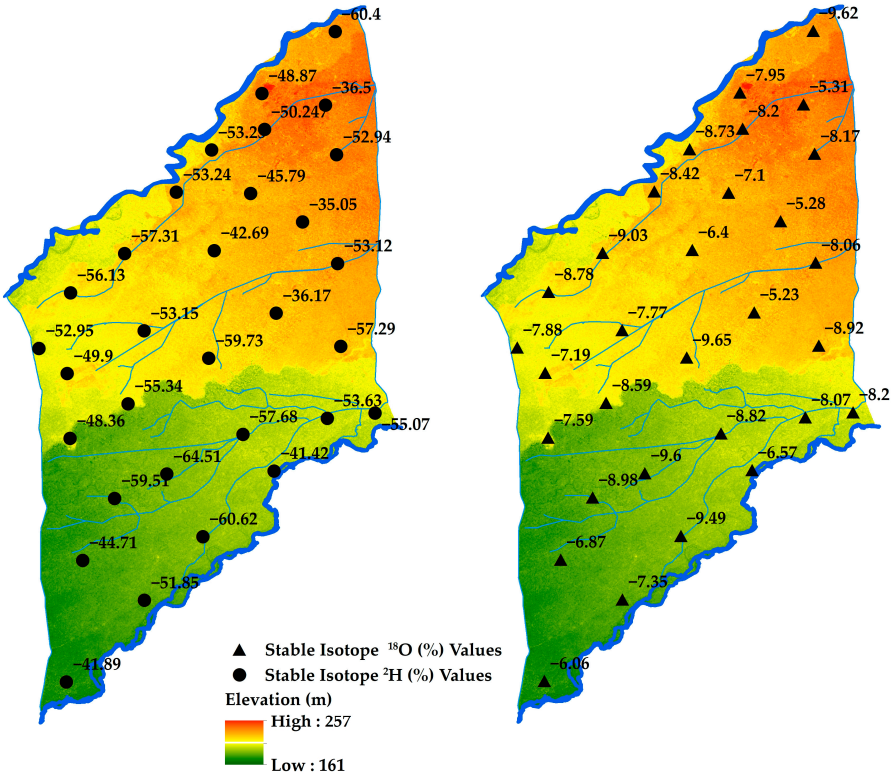

Figure 6. Distribution of stable isotopes by considering elevation of recharge.

4. Discussion

4.1. Climate Ascription to Groundwater Age

The spatial variation of mean monthly rainfall is heterogeneous, and it decreases from east to west (Figure 7a), although mean monthly *Tmax* and *Tmin* increases from east to west (Figure 7b,c). A similar trend was found in the literature [55,56]. Spatial analysis revealed that rainfall is high and temperature is low in eastern side of the study area. As a result, there is a higher availability of water for infiltration and a reduced amount of evapotranspiration from the soil, and, consequently, young groundwater can be present in this area. However, old groundwater is also present in this area, as shown in Figure 3b. This is due to high pumpage and poor infiltration because of the presence of urban area and pavement in cities. This abstraction and overexploitation of groundwater gave the old groundwater an increased presence. In comparison, the western side rainfall is low and temperature is high, and, consequently, old groundwater can be present in this area. Figure 3a shows the presence of younger groundwater in this area. It was also observed that the agriculture area is present on the western side, as presented in Figure 2c, which shows that greater use of irrigation water causes greater infiltration into the soil [57]. This infiltration water caused the presence of young groundwater in western region, as shown in Figure 3b.

4.2. Anthropogenic Factors Attribution with Groundwater Quality and DWT Trends

Chemical parameters are critical factors in understanding the general hydro-geochemistry of the study region. The minimum, maximum, and mean values of EC, SAR, RSC, and DWT are given in Table 4. A considerable difference in maximum and minimum values in water quality parameters and depth to the water table describes the area's heterogeneity.

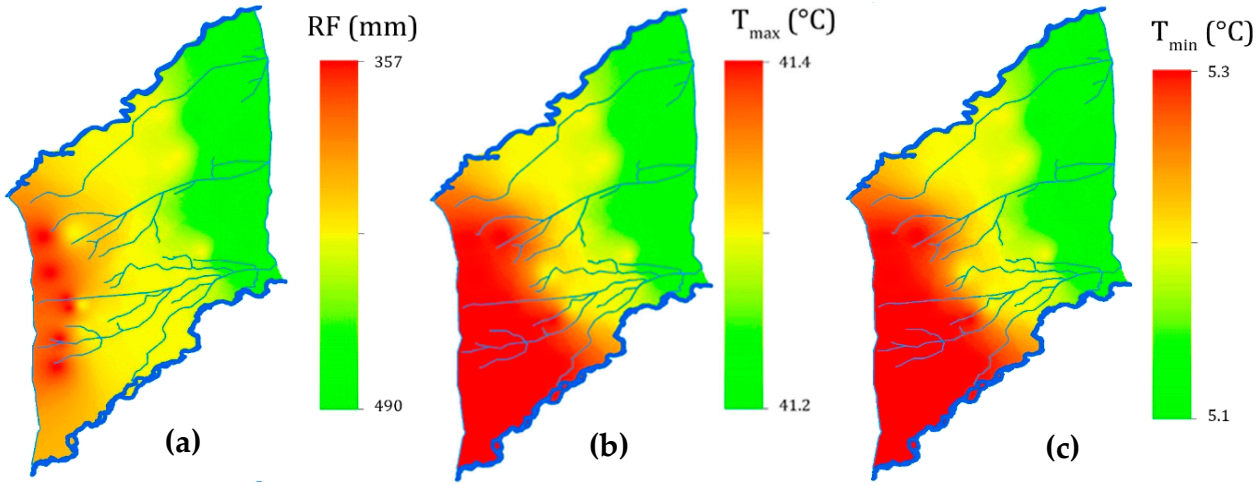

Figure 7. Spatial variation in (**a**) precipitation, (**b**) *Tmax*, and (**c**) *Tmin*.

Table 4. Statistics of groundwater quality parameters.

Parameters	Minimum	Maximum	Mean	Standard Deviation
EC (µS/cm)	400	3000	1392	527.79
SAR (%)	1.10	35.10	10.17	5.58
RSC (mEq/L)	0.40	15.90	4.25	2.73
DWT (meter)	2.8	27.7	13.1	7.62

The MK test was utilized to investigate heterogeneity and examine the trends in groundwater quality parameters and DWT within the study region. The area where EC values in groundwater are increasing has an average rising trend of 14.03 µS/cm per annum (shown in Figure 8a). Based on the findings shown in Figure 9, it was revealed that there is a notable increase in EC values in 63% of the area, while a remarkable decrease in EC values was observed in 35% of the area. However, no discernible trend was detected for the remaining 2% of the area throughout the study period, as shown in Figure 9a,b. EC is continuously increasing in urban areas, (Figure 9a). The EC values also have a rising trend in agricultural areas but are declining in areas near water bodies like rivers (Figure 9b).

In the area where a rising trend was observed, the SAR increases at a mean rate of 0.187% per year. Conversely, in the area where a declining trend was observed, the SAR decreases at a mean rate of 0.04% per year. Overall, SAR values increase at a rate of 0.127% per year (as presented in Figure 8b). Additionally, a significant declining trend was observed in 33% of the area, while a remarkable rising trend was observed in 48% of the area, However, in 19% of the area, no discernible trend was observed in SAR values (as presented in Figure 9c,d). The increasing SAR in populated areas (as presented in Figure 9c) reveals that human activities strongly impact the SAR. SAR values near rivers or canals showed either no trend or a declining trend, while SAR values in areas with limited human population, particularly in agricultural areas and woodlands, also exhibited no trend (Figure 9d).

On average, RSC values are rising at a rate of 0.178 mEq/L per annum (presented in Figure 8c). In 15% of the area, there is no discernible trend in RSC values. However, in 40% of the area, there is a remarkable increasing trend in RSC values, while in 45% of the area, there are significant decreasing trends, as depicted in Figure 8. The impact of human population on RSC is negligible, as it consistently decreases in densely populated areas, (shown in Figure 9e). Additionally, the presence of river water has a positive effect on RSC, as it remains stable or decreases near rivers and in agricultural areas, (as depicted in Figure 9f).

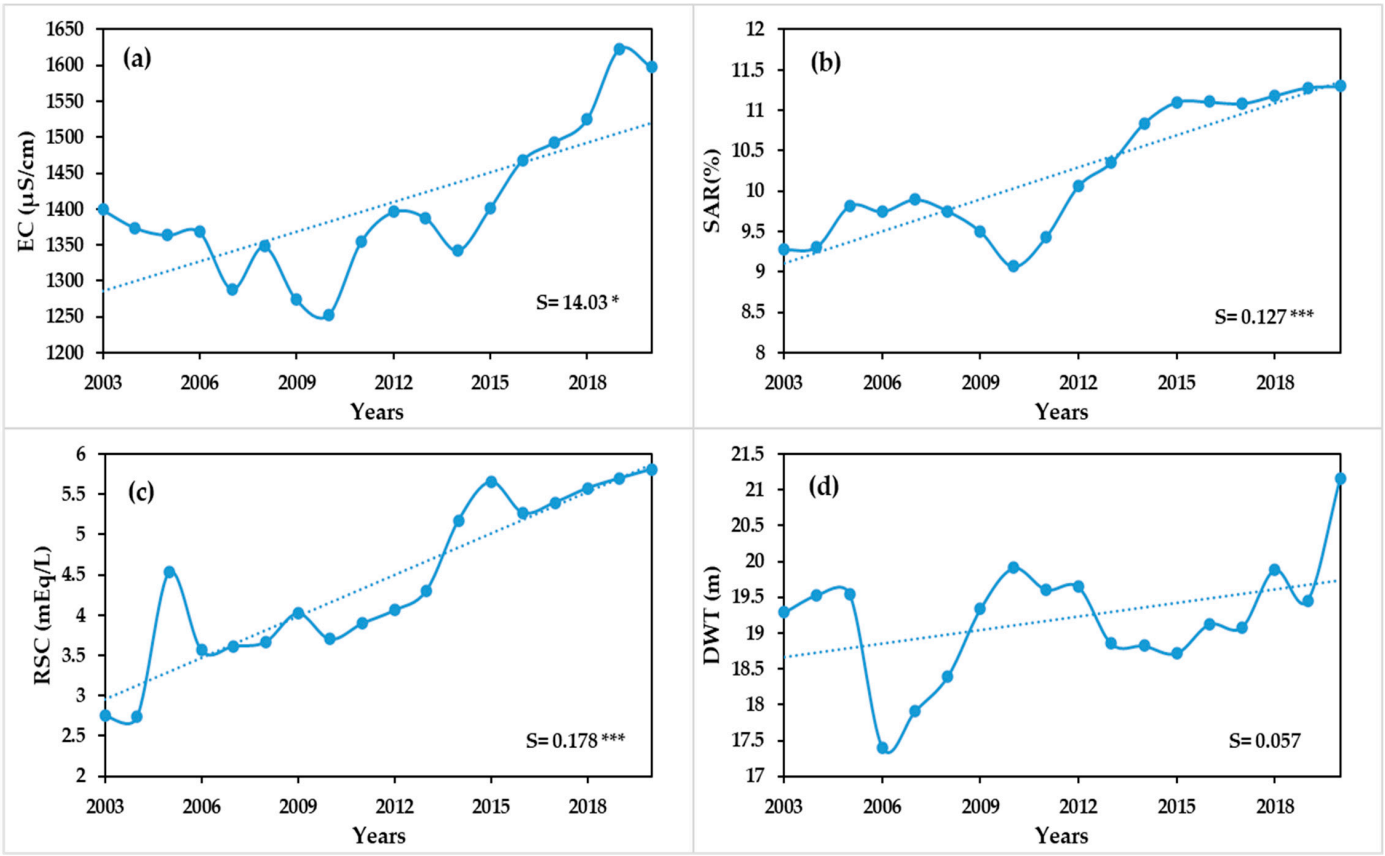

Figure 8. Temporal variation in (**a**) EC (**b**) SAR, (**c**) RSC, and (**d**) DWT. Single (*) and triple (***) asterisk signs represent the significance of trends at 10% and 1% significance level, respectively.

The increase in EC and SAR values is largely dependent on anthropogenic activities. In urban areas, EC levels are continuously rising. However, despite this, the human population tends to settle near rivers, and the continuous recharge of river water leads to an improvement in the quality of groundwater. In Punjab, Pakistan, the rivers have a relatively low EC range of 250–310 µS/cm, and the process of recharging river water enhances the EC of the existing groundwater in the aquifer [58]. The overall trends in water quality parameters improved water quality in the areas near the rivers. As the distance from the river increases, water quality vigor decreases. Moreover, the human population also has a substantial impact on groundwater quality. Anthropogenic activities deteriorate groundwater resources, which needs to be addressed because they affect the sustainability of the local ecosystem [59,60].

Across the study area, the depletion rate is about 0.057 m per year. Spatiotemporal variation in DWT is presented in Figure 9g,h. DWT is affected by different types of anthropogenic activities, mostly by agricultural activities and urbanization. The DWT in urban areas is declining rapidly due to excessive abstraction and impermeable pavement in cities. Although the urban area lies east of the river Ravi, the river recharges the groundwater in this region. The average annual rainfall is also higher in this area, so more rainwater is available to replenish the aquifer. The maximum rate of decline in DWT is 0.15 m/year in urban areas, which is the highest in the whole study area, as presented in Figure 9g. The DWT is declining in agriculture, mainly due to excessive groundwater abstraction. The maximum rate of decline in agricultural areas is 0.091 m/year.

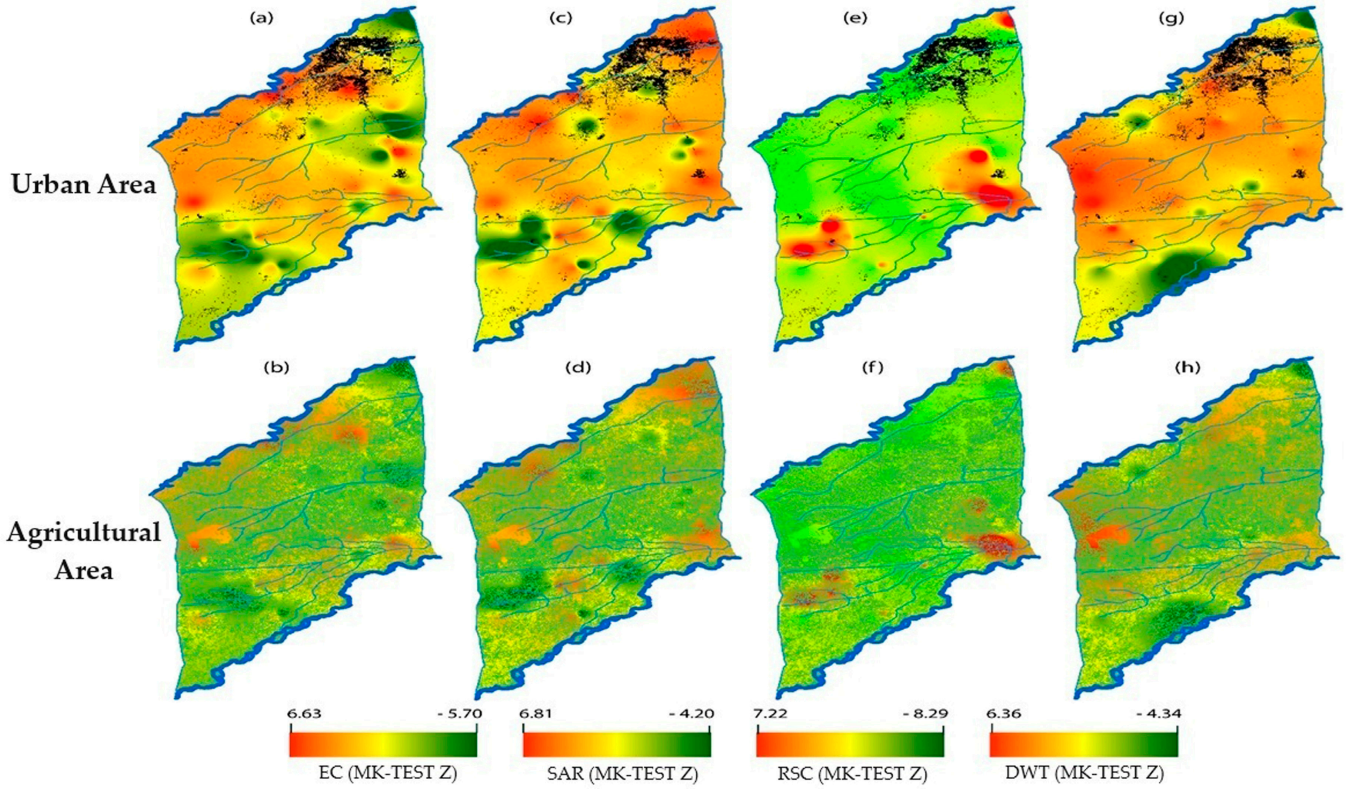

Figure 9. Spatial variation in EC (**a**,**b**), SAR (**c**,**d**), RSC (**e**,**f**), and DWT (**g**,**h**) over urban areas and agricultural areas.

The depth of the water table and groundwater quality are continuously deteriorating in most regions [61]. The DWT is declining because the rate of abstraction is higher than the rate of recharge. The region has witnessed a substantial extraction of groundwater, primarily driven by the continuous rise in the number of agricultural tubewells. In province Punjab, the density of agricultural tubewells has increased exponentially, notably reaching 2000 times higher between 1961 and 2021 [62]. In the study area, Lahore is a metropolitan city, and its population is around 11 million [63]. All the municipal water requirements in Lahore and Kasur city are fulfilled by installing a 120–220 m deep tubewell [64]. The aquifer is under stress, leading to a decline in DWT. The ongoing changes in agriculture and urban development further impact the DWT, causing a continuous decrease in DWT both in densely populated areas and agricultural regions [58,65].

4.3. Anthropogenic Factors Attribution with Groundwater Age and Origin

The age of groundwater in most areas ranges from 10 to 50 years. In the areas near the river and where rainfall contributes to recharge, the groundwater is relatively young at around 5 to 10 years old.

The variation in stable isotopes in groundwater can exhibit differences between urban and agricultural areas, as presented in Figure 10a,b. Lighter stable isotopes were found in urban areas, and this can be attributed to various factors associated with human activities, like a higher concentration of impervious surfaces, such as houses, buildings and bridges, which restrict the infiltration of water into the ground. Consequently, there are fewer opportunities for heavy isotopic fractions present in rainwater during recharge, resulting in a higher proportion of river water containing lighter isotopes infiltrating the groundwater.

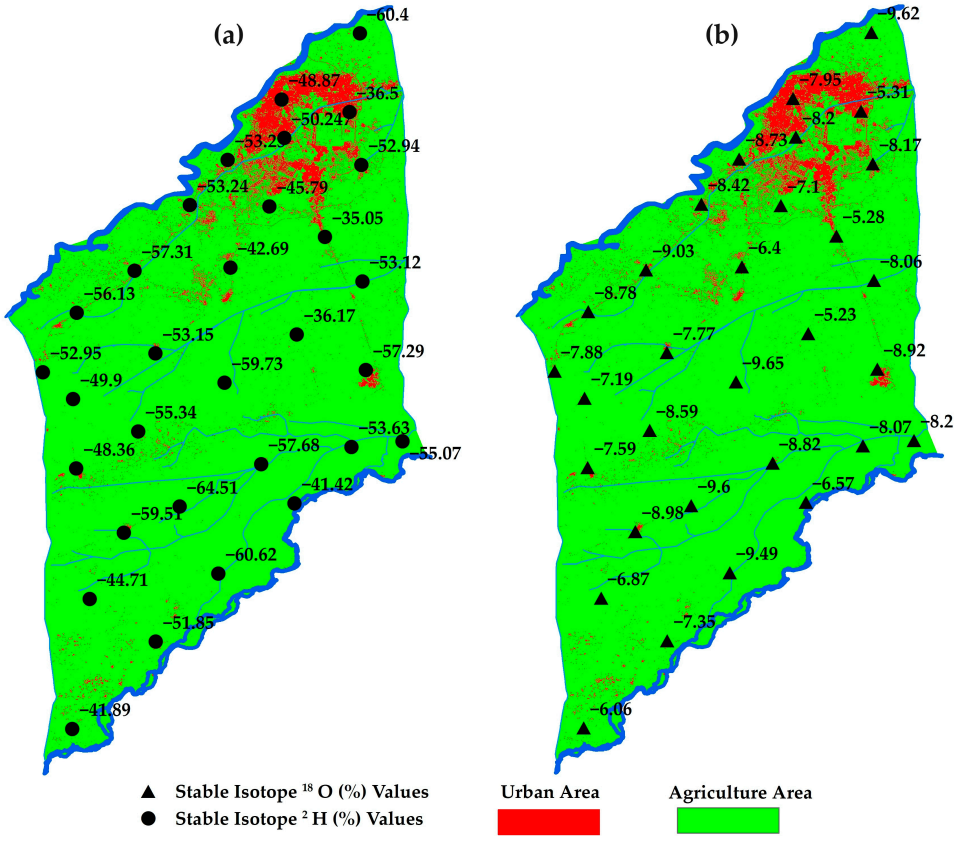

Figure 10. Spatial variation in stable isotope over urban areas and agricultural areas (**a**) ^{2}H (**b**) ^{18}O.

In contrast, groundwater in agricultural areas contain both heavy and light isotopes, as presented in Figure 10b. The presence of these isotopes influenced mainly by irrigation practices either by diverting canal water or using rainwater. Heavy isotopes enter groundwater through precipitation. The presence of rainfall and young groundwater in agricultural areas indicate the rainfall is contributing to recharge. Canal and river water play a critical role in recharging the aquifer of agricultural areas through irrigation. The whole area is mainly irrigated by the diversion of river water through canals, which contain light stable isotopes. Additionally, 20–45.5% of irrigation water is lost, mainly due to seepage [66]. The seepage of irrigation water replenishes groundwater levels by allowing water to infiltrate into the surrounding soil and eventually reach the groundwater. This process introduces young water into the aquifer system, which can potentially impact the age of the groundwater and lead to a decrease in its overall age.

The oldest water was found in the urban area of Lahore city, which is more than 50 years old. The predicted groundwater age indicated that the aquifer in urban areas is over-exploited and under stress. Moreover, old water in urban areas means that high runoff, concrete structures, pavement in urban areas, or low flows in rivers and canals do not recharge the aquifer. A few studies in different countries also reported similar results [67–69]. The study also examined the evolution of groundwater resources, with the main source of recharge being river water, while rainwater contributes less to aquifer recharge. The absence of rainwater in groundwater can occur when there is rapid runoff or when the aquifer is under stress due to excessive groundwater extraction. Moreover, the area with gentle slope and predominantly alluvial soil receives an average annual rainfall of 423 mm. As a result, the volume of rainwater is significant, but it takes a considerable amount of time to infiltrate into the ground. The primary reason for the lack of rainwater recharge is the growth in population, which leads to increased groundwater abstraction and decreased rainwater recharge. The years between 1999 and 2011 saw a doubling of population growth and tripling of urban infrastructure expansion [64]. This makes the

groundwater conditions unsustainable in urban areas because it hinders the rainwater's ability to contribute to the groundwater. Due to construction and concrete pavements in urban areas, rainwater causes urban flooding rather than recharging groundwater [66]. Furthermore, there is a growing focus on urban flooding in urban areas of Lahore and its surroundings, primarily due to the rapid expansion of residential areas and the dense infrastructure within the city. The situation in urban areas is concerning, highlighting the need for rainwater harvesting and an increase in rainwater recharge, particularly in cities and adjacent areas. This situation clearly demonstrates the alarming situation when only river water is present in the urban aquifer, which highlights the need for immediate action to address the issue.

5. Conclusions and Future Scope

This study investigates groundwater origin and age by using stable and radioactive isotopes for aquifer sustainability. The effects of anthropogenic and climatic factors were also attributed to groundwater evaluation. The important conclusions are the following:

- An identified significant amount of river flows replenishes groundwater resources and improves water quality.
- The stable isotopic composition (^{18}O and ^{2}H) of groundwater indicates that river flow and precipitation are the primary sources of groundwater recharge. Additionally, it demonstrates that the recharge area exhibits a higher level of depletion than the discharge area.
- Groundwater is 5–10 years old in 55% of the total area, mainly in woodland and agricultural areas; 10–50-year-old groundwater present in agricultural and urban areas comprises 40% of total areas, and 5% of the area in urban areas contains groundwater more than 50 years old, which demonstrates that urban areas are not receiving recharging water and of the groundwater situation here is unsustainable.
- The water table depth is declining, with a mean rate of 0.057 m/year. This significant decline in water is because of the over-exploitation of groundwater resources.
- The deterioration in the quality of groundwater in the study area has increased from the agricultural and domestic effluents, which makes the water unfit for drinking and irrigation purposes.

This study provides a new perspective in evaluating groundwater resources, which may be helpful in policy-making and sustainable groundwater management. In this study, only a few isotopes, like ^{3}H, ^{2}H, and ^{18}O, were used to examine the age and origin of groundwater. Other isotopes like ^{14}C, ^{36}Cl, ^{85}Kr, and ^{6S}F would be used to track groundwater movement and provide helpful information on groundwater dating. Efficient and micro irrigation methods should be introduced to grow high-value crops. In this study, only NDVI was used to characterize land characteristics of the study area. Future studies should incorporate the cropping pattern with groundwater management through isotope analysis. The understanding of surface and groundwater interaction at a basin scale might be improved by the careful examination of the geology and hydrogeology at a lower scale.

Author Contributions: All authors were involved in the intellectual elements of this paper. U.I. and G.N. designed the research. U.I. and M.I. conducted the research and wrote the manuscript. M.I., M.M., A.B.A., M.S. (Muhammad Saifullah) and M.S. (Muhammad Shahid) helped in the analysis. M.I. reviewed and edited the manuscript in light of reviewers' comments. All authors have read and agreed to the published version of the manuscript.

Funding: This research received no external funding.

Data Availability Statement: The data used in this study includes spatial data, isotopic data of precipitation, and water bodies. This is freely available and can be accessed from the websites given in the data section of the manuscript. The isotopic data on groundwater is the property of the Center of Excellence in Water Resources Engineering (CEWRE), Lahore, and the Pakistan Council of Research in Water Resources (PCRWR), which can be retrieved by making a request to the corresponding

author. However, the climatic data is the property of the Pakistan Meteorological Department (PMD) and can be requested via official channels.

Acknowledgments: The authors are grateful to the Center of Excellence in Water Resources Engineering (CEWRE), Lahore, and Pakistan Institute of Nuclear Science and Technology (PINSTECH), Pakistan for supporting financially and conducting the laboratory work. The authors are also thankful to the Pakistan Council of Research in Water Resources (PCRWR) for providing the analysis of isotopes data.

Conflicts of Interest: The authors declare no conflict of interest.

References

1. Li, C.; Odermatt, D.; Bouffard, D.; Wüest, A.; Kohn, T. Coupling Remote Sensing and Particle Tracking to Estimate Trajectories in Large Water Bodies. *Int. J. Appl. Earth Obs. Geoinf.* **2022**, *110–118*, 102809. [CrossRef]
2. Kumar, C.P. Climate Change and Its Impact on Groundwater Resources. *Int. J. Eng. Sci.* **2012**, *1*, 43–60.
3. Huang, G.; Sun, J.; Zhang, Y.; Chen, Z.; Liu, F. Impact of Anthropogenic and Natural Processes on the Evolution of Groundwater Chemistry in a Rapidly Urbanized Coastal Area, South China. *Sci. Total Environ.* **2013**, *463*, 209–221. [CrossRef] [PubMed]
4. Earman, S.; Dettinger, M. Potential Impacts of Climate Change on Groundwater Resources—A Global Review. *J. Water Clim. Change* **2011**, *2*, 213–229. [CrossRef]
5. Jiang, Y.; Wu, Y.; Groves, C.; Yuan, D.; Kambesis, P. Natural and Anthropogenic Factors Affecting the Groundwater Quality in the Nandong Karst Underground River System in Yunan, China. *J. Contam. Hydrol.* **2009**, *109*, 49–61. [CrossRef] [PubMed]
6. Bahir, M.; El Mountassir, O.; Dhiba, D.; Chehbouni, A.; Carreira, P.M.; Elbiar, H. Combining Stable Isotope and WQI Methods to Study the Groundwater Quality: A Case Study in Essaouira City, Morocco. *SN Appl. Sci.* **2022**, *4*, 317–329. [CrossRef] [PubMed]
7. Guo, X.; Zuo, R.; Meng, L.; Wang, J.; Teng, Y.; Liu, X.; Chen, M. Seasonal and Spatial Variability of Anthropogenic and Natural Factors Influencing Groundwater Quality Based on Source Apportionment. *Int. J. Environ. Res. Public Health* **2018**, *15*, 279. [CrossRef]
8. Bretzler, A.; Osenbrück, K.; Gloaguen, R.; Ruprecht, J.S.; Kebede, S.; Stadler, S. Groundwater Origin and Flow Dynamics in Active Rift Systems—A Multi-Isotope Approach in the Main Ethiopian Rift. *J. Hydrol.* **2011**, *402*, 274–289. [CrossRef]
9. Kebede, S.; Travi, Y.; Asrat, A.; Alemayehu, T.; Ayenew, T.; Tessema, Z. Groundwater Origin and Flow along Selected Transects in Ethiopian Rift Volcanic Aquifers. *Hydrogeol. J.* **2008**, *16*, 55–73. [CrossRef]
10. Smerdon, B.D.; Gardner, W.P. Characterizing Groundwater Flow Paths in an Undeveloped Region through Synoptic River Sampling for Environmental Tracers. *Hydrol. Process.* **2022**, *36*, 130–145. [CrossRef]
11. Gleeson, T.; Befus, K.M.; Jasechko, S.; Luijendijk, E.; Cardenas, M.B. The Global Volume and Distribution of Modern Groundwater. *Nat. Geosci.* **2016**, *9*, 161–164. [CrossRef]
12. Adomako, D.; Maloszewski, P.; Stumpp, C.; Osae, S.; Akiti, T.T. Estimating groundwater recharge from water isotope (δ2H, δ18O) depth profiles in the Densu River basin, Ghana. *Hydrol. Sci. J.* **2010**, *55*, 1405–1416. [CrossRef]
13. Abbott, M.D.; Lini, A.; Bierman, P.R. δ18O, δD and 3H Measurements Constrain Groundwater Recharge Patterns in an Upland Fractured Bedrock Aquifer, Vermont, USA. *J. Hydrol.* **2000**, *228*, 101–112. [CrossRef]
14. Bedaso, Z.K.; Wu, S.Y.; Johnson, A.N.; McTighe, C. Assessing Groundwater Sustainability under Changing Climate Using Isotopic Tracers and Climate Modelling, Southwest Ohio, USA. *Hydrol. Sci. J.* **2019**, *64*, 798–807. [CrossRef]
15. Jasechko, S.; Birks, S.J.; Gleeson, T.; Wada, Y.; Fawcett, P.J.; Sharp, Z.D.; McDonnell, J.J.; Welker, J.M. The Pronounced Seasonality of Global Groundwater Recharge. *Water Resour. Res.* **2014**, *50*, 8845–8867. [CrossRef]
16. Abiye, T.A.; Mengistu, H.; Masindi, K.; Demlie, M. Surface Water and Groundwater Interaction in the Upper Crocodile River Basin Johannesburg, South Africa: Environmental Isotope Approach. *S. Afr. J. Geol.* **2015**, *118*, 109–118. [CrossRef]
17. Castro, M.C.; Goblet, P. Calculation of Ground Water Ages—A Comparative Analysis. *Ground Water* **2005**, *43*, 368–380. [CrossRef]
18. Stefánsson, A.; Arnórsson, S.; Sveinbjörnsdóttir, Á.E.; Heinemaier, J.; Kristmannsdóttir, H. Isotope (ΔD, Δ18O, 3H, Δ13C, 14C) and Chemical (B, Cl) Constrains on Water Origin, Mixing, Water-Rock Interaction and Age of Low-Temperature Geothermal Water. *Appl. Geochem.* **2019**, *108–119*, 104380. [CrossRef]
19. Zhu, B.Q.; Ren, X.Z.; Rioual, P. Geological Control on the Origin of Fresh Groundwater in the Otindag Desert, China. *Appl. Geochem.* **2019**, *103*, 131–142. [CrossRef]
20. Jin, K.; Rao, W.; Tan, H.; Song, Y.; Yong, B.; Zheng, F.; Chen, T.; Han, L. H-O Isotopic and Chemical Characteristics of a Precipitation-Lake Water-Groundwater System in a Desert Area. *J. Hydrol.* **2018**, *559*, 848–860. [CrossRef]
21. Zhao, J.B.; Ma, Y.D.; Luo, X.Q.; Yue, D.P.; Shao, T.J.; Dong, Z.B. The Discovery of Surface Runoff in the Megadunes of Badain Jaran Desert, China, and Its Significance. *Sci. China Earth Sci.* **2017**, *60*, 707–719. [CrossRef]
22. Wu, X.; Wang, X.S.; Wang, Y.; Hu, B.X. Origin of Water in the Badain Jaran Desert, China: New Insight from Isotopes. *Hydrol. Earth Syst. Sci.* **2017**, *21*, 4419–4431. [CrossRef]
23. Rahul, P.; Prasanna, K.; Ghosh, P.; Anilkumar, N.; Yoshimura, K. Stable Isotopes in Water Vapor and Rainwater over Indian Sector of Southern Ocean and Estimation of Fraction of Recycled Moisture. *Sci. Rep.* **2018**, *8*, 7552–7562. [CrossRef] [PubMed]
24. Müller, T.; Friesen, J.; Weise, S.M.; Al Abri, O.; Bait Said, A.B.A.; Michelsen, N. Stable Isotope Composition of Cyclone Mekunu Rainfall, Southern Oman. *Water Resour. Res.* **2020**, *56*, 1944–1957. [CrossRef]

25. Nicholson, S.L.; Pike, A.W.G.; Hosfield, R.; Roberts, N.; Sahy, D.; Woodhead, J.; Cheng, H.; Edwards, R.L.; Affolter, S.; Leuenberger, M.; et al. Pluvial Periods in Southern Arabia over the Last 1.1 Million-Years. *Quat. Sci. Rev.* **2020**, *229–246*, 106112. [CrossRef]
26. Kisi, O.; Ay, M. Comparison of Mann-Kendall and Innovative Trend Method for Water Quality Parameters of the Kizilirmak River, Turkey. *J. Hydrol.* **2014**, *513*, 362–375. [CrossRef]
27. Farid, H.U.; Ayub, H.U.; Khan, Z.M.; Ahmad, I.; Anjum, M.N.; Kanwar, R.M.A.; Mubeen, M.; Sakinder, P. Groundwater Quality Risk Assessment Using Hydro-Chemical and Geospatial Analysis. *Environ. Dev. Sustain.* **2023**, *25*, 8343–8365. [CrossRef]
28. Douglas, A.A.; Osiensky, J.L.; Keller, C.K. Carbon-14 Dating of Ground Water in the Palouse Basin of the Columbia River Basalts. *J. Hydrol.* **2007**, *334*, 502–512. [CrossRef]
29. McMahon, P.B.; Galloway, J.M.; Hunt, A.G.; Belitz, K.; Jurgens, B.C.; Johnson, T.D. Geochemistry and Age of Groundwater in the Williston Basin, USA: Assessing Potential Effects of Shale-Oil Production on Groundwater Quality. *Appl. Geochem.* **2021**, *125–141*, 104833. [CrossRef]
30. Jasmin, I.; Mallikarjuna, P. Review: Satellite-Based Remote Sensing and Geographic Information Systems and Their Application in the Assessment of Groundwater Potential, with Particular Reference to India. *Hydrogeol. J.* **2011**, *19*, 729–740. [CrossRef]
31. Eraifej, N.; Abu-Jaber, N. Geochemistry and Pollution of Shallow Aquier in the Mofraq Area, Northan Jordan. *Environ. Geol.* **1999**, *37*, 162–170. [CrossRef]
32. Abu-Jaber, N. Geochemical Evolution and Recharge of the Shallow Aquifers at Tulul al Ashaqif, NE Jordan. *Environ. Geol.* **2001**, *41*, 372–383. [CrossRef]
33. Hussain, S.; Xianfang, S.; Hussain, I.; Jianrong, L.; Dong Mei, H.; Li Hu, Y.; Huang, W. Controlling Factors of the Stable Isotope Composition in the Precipitation of Islamabad, Pakistan. *Adv. Meteorol.* **2015**, *2015*, 817513. [CrossRef]
34. Ahmad, M.; Rafiq, M.; Akram, W.; Tasneem, M.A.; Ahmad, N.; Iqbal, N.; Sajjad, M.I. *Assessment of Aquifer System in the City of Lahore, Pakistan Using Isotopic Techniques*; International Atomic Energy Agency: Vienna, Austria, 2002; pp. 109–133.
35. Fahad, S.; Li, W.; Lashari, A.H.; Islam, A.; Khattak, L.H.; Rasool, U. Evaluation of Land Use and Land Cover Spatio-Temporal Change during Rapid Urban Sprawl from Lahore, Pakistan. *Urban. Clim.* **2021**, *39*, 501–518. [CrossRef]
36. Leghari, S.J.; Hu, K.; Wei, Y.; Wang, T.; Bhutto, T.A.; Buriro, M. Modelling Water Consumption, N Fates and Maize Yield under Different Water-Saving Management Practices in China and Pakistan. *Agric. Water Manag.* **2021**, *255–265*, 107033. [CrossRef]
37. Qureshi, A.S.; Gill, M.A.; Sarwar, A. Sustainable Groundwater Management in Pakistan: Challenges and Opportunities. *Irrig. Drain.* **2010**, *59*, 107–116. [CrossRef]
38. Hasan, M.; Shang, Y.; Akhter, G.; Jin, W. Geophysical Assessment of Groundwater Potential: A Case Study from Mian Channu Area, Pakistan. *Groundwater* **2018**, *56*, 783–796. [CrossRef] [PubMed]
39. Birdi, P.K.; Kale, K.V. Accuracy Assessment of Classification on Landsat-8 Data for Land Cover and Land Use of an Urban Area by Applying Different Image Fusion Techniques and Varying Training Samples. In *Microelectronics, Electromagnetics and Telecommunications*; Springer: Singapore, 2019; Volume 521, pp. 189–198. [CrossRef]
40. IAEA. *Sampling and Isotope Analysis of Agricultural Pollutant in Water*; IAEA: Vienna, Austria, 2018; pp. 8–9.
41. Broers, H.P. The Spatial Distribution of Groundwater Age for Different Geohydrological Situations in the Netherlands: Implications for Groundwater Quality Monitoring at the Regional Scale. *J. Hydrol.* **2004**, *299*, 84–106. [CrossRef]
42. Gusyev, M.A.; Abrams, D.; Toews, M.W.; Morgenstern, U.; Stewart, M.K.; Hutt, L.; Zealand, N.; Survey, S.W.; Dynamics, A.; Hutt, L.; et al. A Comparison of Particle-Tracking and Solute Transport Methods for Simulation of Tritium Concentrations and Groundwater Transit Times in River Water. *Hydrol. Earth Syst. Sci.* **2014**, *18*, 3109–3119. [CrossRef]
43. Franck, D.; Asselineau, B.; Carlan, L.D.E.; Clairand, I.; Huet, C.; Lacoste, V.; Trompier, F. La Dosimétrie à l ' IRSN. *Radioprotection* **2007**, *41*, 227–252. [CrossRef]
44. Beyerle, U.; Aeschbach-Hertig, W.; Imboden, D.M.; Baur, H.; Graf, T.; Kipfer, R. A Mass, Spectrometric System for the Analysis of Noble Gases and Tritium from Water Samples. *Environ. Sci. Technol.* **2000**, *34*, 2042–2050. [CrossRef]
45. Singh, R.P.; Singh, N.; Singh, S.; Mukherjee, S. Normalized Difference Vegetation Index (NDVI) Based Classification to Assess the Change in Land Use/Land Cover (LULC) in Lower Assam, India. *Int. J. Adv. Remote Sens. GIS* **2016**, *5*, 1963–1970. [CrossRef]
46. Gao, W.; Zheng, C.; Liu, X.; Lu, Y.; Chen, Y.; Wei, Y.; Ma, Y. NDVI-Based Vegetation Dynamics and Their Responses to Climate Change and Human Activities from 1982 to 2020: A Case Study in the Mu Us Sandy Land, China. *Ecol. Indic.* **2022**, *137*, 229–243. [CrossRef]
47. Roznik, M.; Boyd, M.; Porth, L. Improving Crop Yield Estimation by Applying Higher Resolution Satellite NDVI Imagery and High-Resolution Cropland Masks. *Remote Sens. Appl.* **2022**, *25*, 713–726. [CrossRef]
48. Taufik, A.; Sakinah, S.; Ahmad, S.; Ahmad, A. Classification of Landsat 8 Satellite Data Using NDVI Thresholds. *J. Telecommun. Electron. Comput. Eng.* **2016**, *8*, 401–405.
49. Mann, H.B. Nonparametric Tests against Trend. *Econometrica* **1945**, *13*, 245–259. [CrossRef]
50. Kendall, M. *Rank Correlation Methods*, 4th ed.; Charles Griffin: London, UK, 1975.
51. Hamed, K.H. Trend Detection in Hydrologic Data: The Mann-Kendall Trend Test under the Scaling Hypothesis. *J. Hydrol.* **2008**, *349*, 350–363. [CrossRef]
52. Sutton, C.; Kumar, S.; Lee, M.K.; Davis, E. Human Imprint of Water Withdrawals in the Wet Environment: A Case Study of Declining Groundwater in Georgia, USA. *J. Hydrol. Reg. Stud.* **2021**, *35*, 401–417. [CrossRef]
53. Helsel, D.R.; Hirsch, R.M. *Statistical Methods in Water Resources*; Elsevier: Amsterdam, The Netherlands, 1992; pp. 119–129.

54. Jasechko, S. *Global Isotope Hydrogeology—Review. Reviews of Geophysics*; Blackwell Publishing Ltd.: Hoboken, NJ, USA, 2019; pp. 835–965. [CrossRef]
55. Varikoden, H.; Revadekar, J.V. On the Extreme Rainfall Events during the Southwest Monsoon Season in Northeast Regions of the Indian Subcontinent. *Meteorol. Appl.* **2020**, *27*, 227–240. [CrossRef]
56. Jiang, X.; Ting, M. A Dipole Pattern of Summertime Rainfall across the Indian Subcontinent and the Tibetan Plateau. *J. Clim.* **2017**, *30*, 9607–9620. [CrossRef]
57. Tanachaichoksirikun, P.; Seeboonruang, U. Distributions of Groundwater Age under Climate Change of Thailand's Lower Chao Phraya Basin. *Water* **2020**, *12*, 3474. [CrossRef]
58. Qadir, A.; Malik, R.N.; Husain, S.Z. Spatio-Temporal Variations in Water Quality of Nullah Aik-Tributary of the River Chenab, Pakistan. *Environ. Monit. Assess.* **2008**, *140*, 43–59. [CrossRef] [PubMed]
59. James, M.; Ren, Z.; Peterson, T.J.; Chen, D. Water Table Depth Data for Use in Modelling Residential Building Ground-Coupled Heat Transfer. *Clean. Eng. Technol.* **2021**, *3*, 221–229. [CrossRef]
60. Brkić, Ž.; Larva, O.; Kuhta, M. Groundwater Age as an Indicator of Nitrate Concentration Evolution in Aquifers Affected by Agricultural Activities. *J. Hydrol.* **2021**, *602–620*, 126799. [CrossRef]
61. Mehmood, Z.; Khan, N.M.; Sadiq, S.; Mandokhail, S.; Ullah, J.; Ashiq, S.Z. Assessment of Subsurface Lithology, Groundwater Depth, and Quality of UET Lahore, Pakistan, Using Electrical Resistivity Method. *Arab. J. Geosci.* **2020**, *13*, 281–288. [CrossRef]
62. Awais, M.; Arshad, M.; Ahmad, S.R.; Nazeer, A.; Waqas, M.M.; Aziz, R.; Shakoor, A.; Rizwan, M.; Chauhdary, J.N.; Mehmood, Q.; et al. Simulation of Groundwater Flow Dynamics under Different Stresses Using MODFLOW in Rechna Doab, Pakistan. *Sustainability* **2023**, *15*, 661. [CrossRef]
63. Zia, S.; Shirazi, S.A.; Nasar-U-Minallah, M. Vulnerability Assessment of Urban Floods in Lahore, Pakistan Using GIS Based Integrated Analytical Hierarchy Approach. *Proc. Pak. Acad. Sci. USA* **2021**, *58*, 85–96. [CrossRef]
64. Ahmad, I.; Saleem, S. Lahore, Pakistan—Urbanization Challenges and Opportunities. *Cities* **2017**, *72*, 348–355. [CrossRef]
65. Zakir-hassan, G.; Shabir, G.; Hassn, F.R.; Akhtar, S. Groundwater-Food Security Nexus under Changing Climate-Historical Prospective of Indus Basin Irrigation System In Pakistan. *Int. J. Soc. Sci. Humanit. Res.* **2022**, *5*, 28–38.
66. Shah, Z.; Gabriel, H.; Haider, S.; Jafri, T. Analysis of Seepage Loss from Concrete Lined Irrigation Canals in Punjab, Pakistan. *Irrig. Drain.* **2020**, *69*, 668–681. [CrossRef]
67. Okuhata, B.K.; Thomas, D.M.; Dulai, H.; Popp, B.N.; Lee, J.; El-Kadi, A.I. Inference of Young Groundwater Ages and Modern Groundwater Proportions Using Chlorofluorocarbon and Tritium/Helium-3 Tracers from West Hawai'i Island. *J. Hydrol.* **2022**, *609*, 277–291. [CrossRef]
68. Casillas-Trasvina, A.; Rogiers, B.; Beerten, K.; Pärn, J.; Wouters, L.; Walraevens, K. Using Helium-4, Tritium, Carbon-14 and Other Hydrogeochemical Evidence to Evaluate the Groundwater Age Distribution: The Case of the Neogene Aquifer, Belgium. *J. Hydrol. X* **2022**, *17–36*, 100132. [CrossRef]
69. Thomas, J.M.; Hershey, R.L.; Fereday, W.; Burr, G. Using Carbon-14 of Dissolved Organic Carbon to Determine Groundwater Ages and Travel Times in Aquifers with Low Organic Carbon. *Appl. Geochem.* **2021**, *124–141*, 104842. [CrossRef]